Electronic Supplementary Material (ESI) for Nanoscale.

Supporting Information

Hydrogen Evolution Reaction Mechanism on Ti_3C_2 MXene Revealed by In-situ/Operando Raman Spectroelectrochemistry

Denis Johnson, Hao-En Lai, Kyle Hansen, Perla Balbuena, and Abdoulaye Djire**

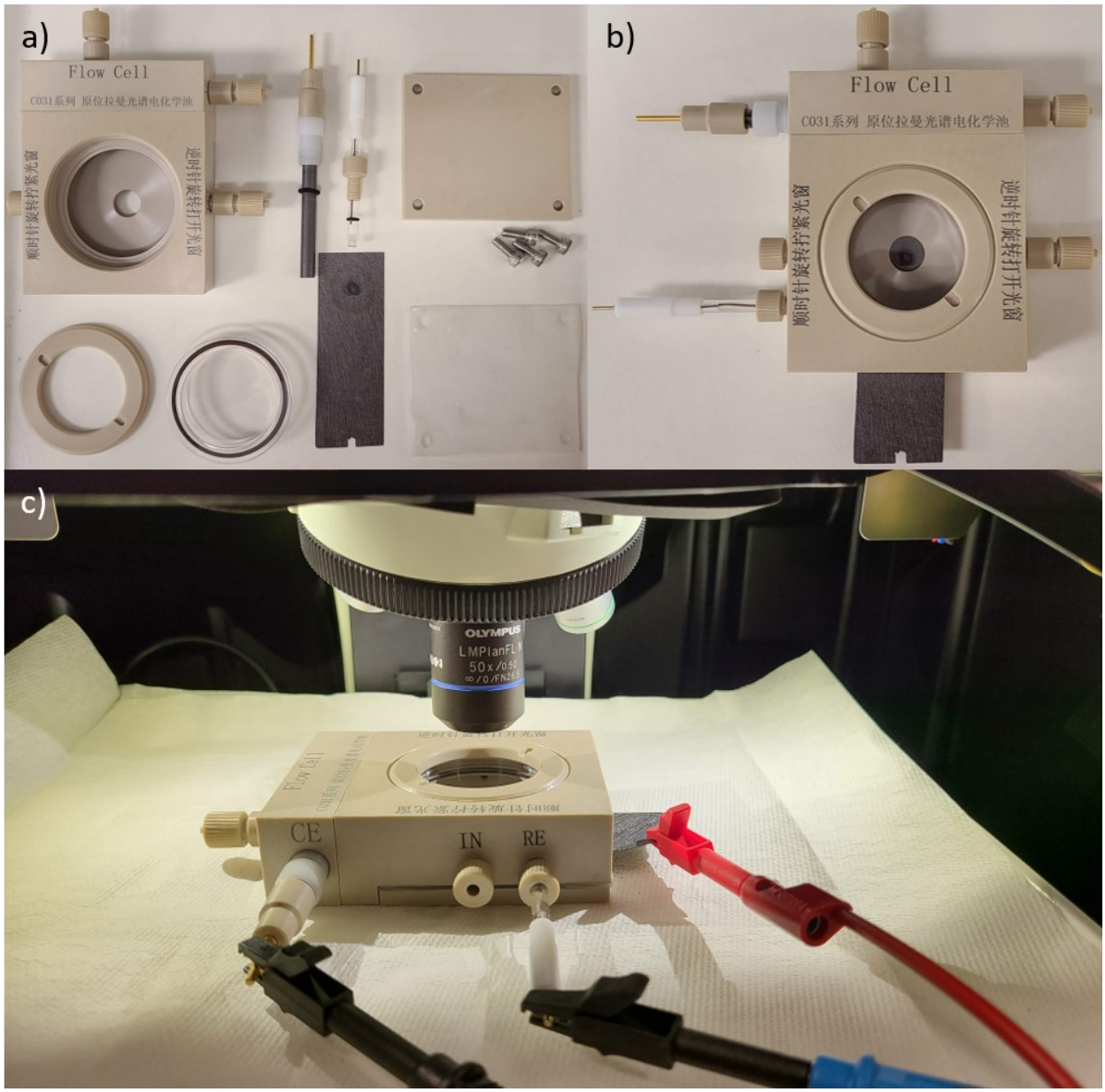

Figure S1. The **a.** disassembled and **b.** assembled view of the in-situ/operando Raman flow cell. **c.** The flow cell assembled, placed under the Raman microscope, and connected to the Potentiostat for data collection.

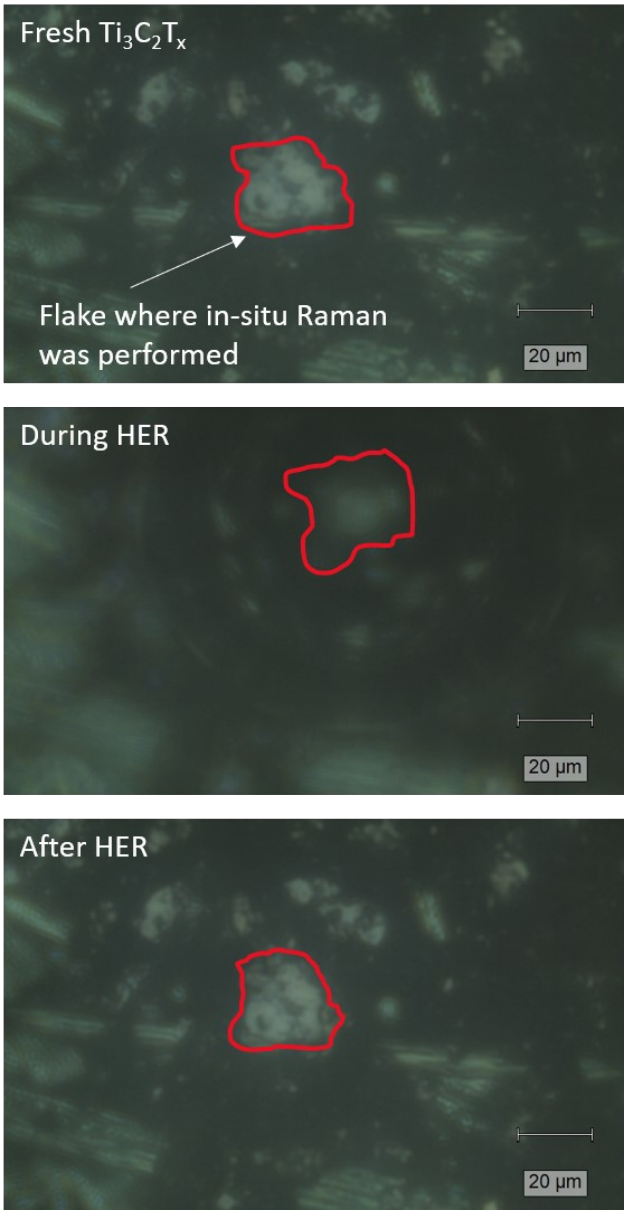

Figure S2. Images of $Ti_3C_2T_x$ MXene flake before, during, and after HER process in acidic electrolyte as viewed through Raman eyepiece.

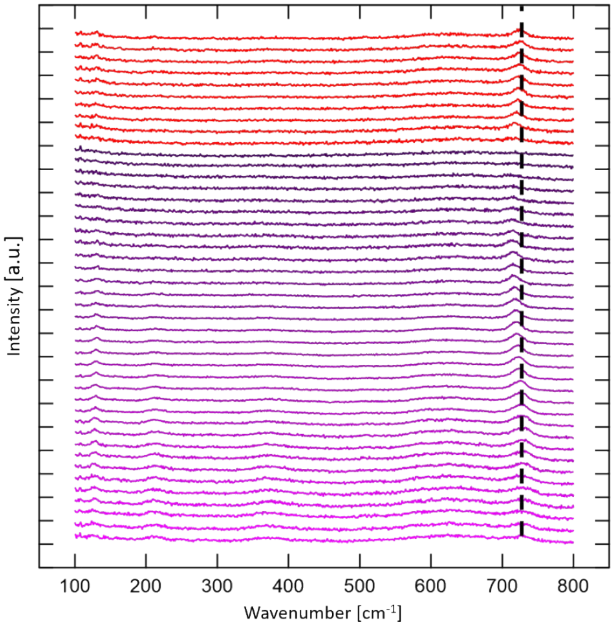

Figure S3. In-situ/operando Raman spectra throughout the HER process in acidic electrolyte. Bottom spectrum corresponds to before HER and moving upward is as more cathodic potential is applied. The dotted line corresponds to the peak at 735 cm^{-1}.

Figure S4. Images of $Ti_3C_2T_x$ MXene flake before, during, and after HER process in neutral electrolyte as viewed through Raman eyepiece.

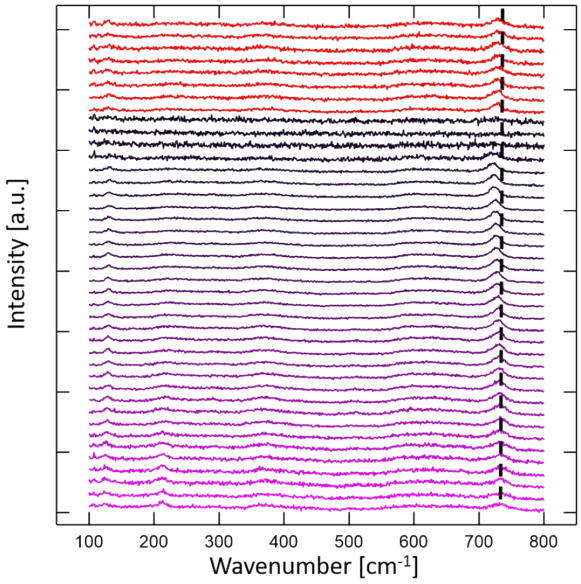

Figure S5. In-situ/operando Raman spectra throughout the HER process in neutral electrolyte. Bottom spectrum corresponds to before HER and moving upward is as more cathodic potential is applied. The dotted line corresponds to the peak at 735 cm^{-1}.

Table S1. c-lattice parameter and interlayer spacing (d-lattice parameter) from DFT optimized structure of neutral charge cell

Structure Formula	Lattice parameter c,	Interlayer parameter, nm	z position of	z position of	Bader atomic	Layer thickness

	nm		bottom atom (Å)	top atom (Å)	radius (Å)	(Å)
			Ti	Ti		
Ti_3C_2	2.292	1.562	9.016	13.881	1.217	7.299
			F	F		
$Ti_3C_2F_2$	2.049	1.271	6.604	12.797	0.794	7.781
			H	H		
Ti3C2O2H2	2.316	1.301	6.867	16.284	0.37	10.157
			O	O		
Ti3C2O2	2.222	1.340	7.513	14.697	0.82	8.824

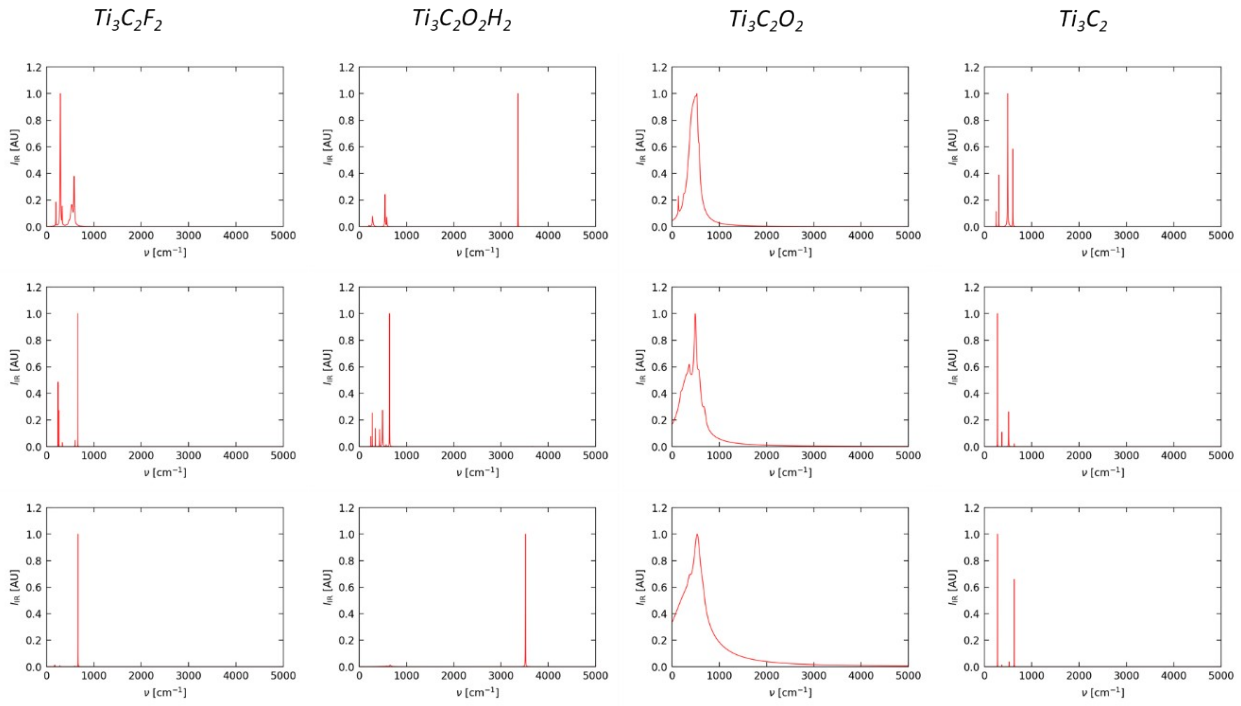

Figure S6. DFT calculated IR spectrum at 300K from the optimized unit cell structure. Linewidths are obtained from a high-quality Phono3py calculation [1]. From left to right: $Ti_3C_2F_2$, $Ti_3C_2O_2H_2$,

$Ti_3C_2O_2$, Ti_3C_2. From top to bottom: oxidation (an electron removed from DFT simulation cell), neutral charge, reduction (an electron added to DFT simulation cell).

Table S2. Highlights from IR spectra for bare Ti_3C_2

Oxidation			Neutral Charge			Reduction		
Ir. Rep.	ν [cm^{-1}]	I [e^2 amu^{-1}]	Ir. Rep.	ν [cm^{-1}]	I [e^2 amu^{-1}]	Ir. Rep.	ν [cm^{-1}]	I [e^2 amu^{-1}]
Bu	306.884	0.086839	Au	277.210	0.376507	Bu	278.038	1.306773
Bu	494.195	0.972596	Bu	277.211	0.376522	Au	278.059	1.306677
Bu	603.705	0.104873	Bu	514.082	0.724299	Bu	524.673	0.461816
Au	603.711	0.10482	Au	631.987	0.024477	Bu	630.795	1.805062

Table S3. Highlights from IR spectra for $Ti_3C_2O_2H_2$

Oxidation			Neutral Charge			Reduction		
Ir. Rep.	ν [cm^{-1}]	I [e^2 amu^{-1}]	Ir. Rep.	ν [cm^{-1}]	I [e^2 amu^{-1}]	Ir. Rep.	ν [cm^{-1}]	I [e^2 amu^{-1}]
Bu	544.752	0.520564	A’	492.842	3.029144	Bu	491.571	3.789274
Bu	582.716	0.857163	A”	642.222	2.113524	Bu	491.704	2.865518
Bu	283.724	1.083679	A’	642.236	2.109906	Au	491.841	1.897722
Au	283.716	1.083707	A’	3651.655	0.809475	Bu	654.838	3.491156
Bu	545.044	1.147183	A’	3666.612	0.951668	Au	655.040	3.497118
Au	545.018	1.147410				Bu	3517.779	65.94866
Bu	3360.582	1.769923						

Table S4. Highlights from IR spectra for $Ti_3C_2O_2$

Oxidation			Neutral Charge			Reduction		
Ir. Rep.	ν [cm^{-1}]	I [e^2	Ir. Rep.	ν [cm^{-1}]	I [e^2	Ir. Rep.	ν [cm^{-1}]	I [e^2

		amu^{-1}]			amu^{-1}]			amu^{-1}]
A	408.759	5.030507	Bu	321.459	11.20945	Au	316.182	4.418034
A	413.489	5.031629	Au	322.387	11.05607	Bu	316.619	4.390141
A	496.593	3.861284	Bu	489.571	1.843076	Bu	534.078	2.485161
A	497.201	3.676383	Au	490.920	1.895808	Au	535.036	2.462244
A	528.447	0.934881	Bu	574.053	2.385487			

Table S5. Highlights from IR spectra for $Ti_3C_2F_2$

Oxidation			Neutral Charge			Reduction		
Ir. Rep.	ν [cm^{-1}]	I [e^2 amu^{-1}]	Ir. Rep.	ν [cm^{-1}]	I [e^2 amu^{-1}]	Ir. Rep.	ν [cm^{-1}]	I [e^2 amu^{-1}]
Au	291.880	1.300046	Au	242.454	0.437698	Bu	173.891	5.757361
Bu	291.896	1.300390	Bu	242.586	0.438243	Au	173.926	5.731884
Bu	532.146	1.107718	Bu	265.803	0.306135	Au	666.927	58.657078
Au	532.143	1.108118	Au	266.112	0.305828	Bu	666.967	58.462026
Bu	583.917	1.238923	Bu	599.664	0.325586			
			Bu	664.535	0.827526			
			Au	664.720	0.828577			

Table S6. Highlights from IR spectra for $Ti_3C_2O(OH)$

Oxidation			Neutral Charge			Reduction		
Ir. Rep.	ν [cm^{-1}]	I [e^2 amu^{-1}]	Ir. Rep.	ν [cm^{-1}]	I [e^2 amu^{-1}]	Ir. Rep.	ν [cm^{-1}]	I [e^2 amu^{-1}]

			A”	275.24	0.42			
			A’	275.34	0.42			
			A’	587.85	1.43			
			A”	587.96	1.43			

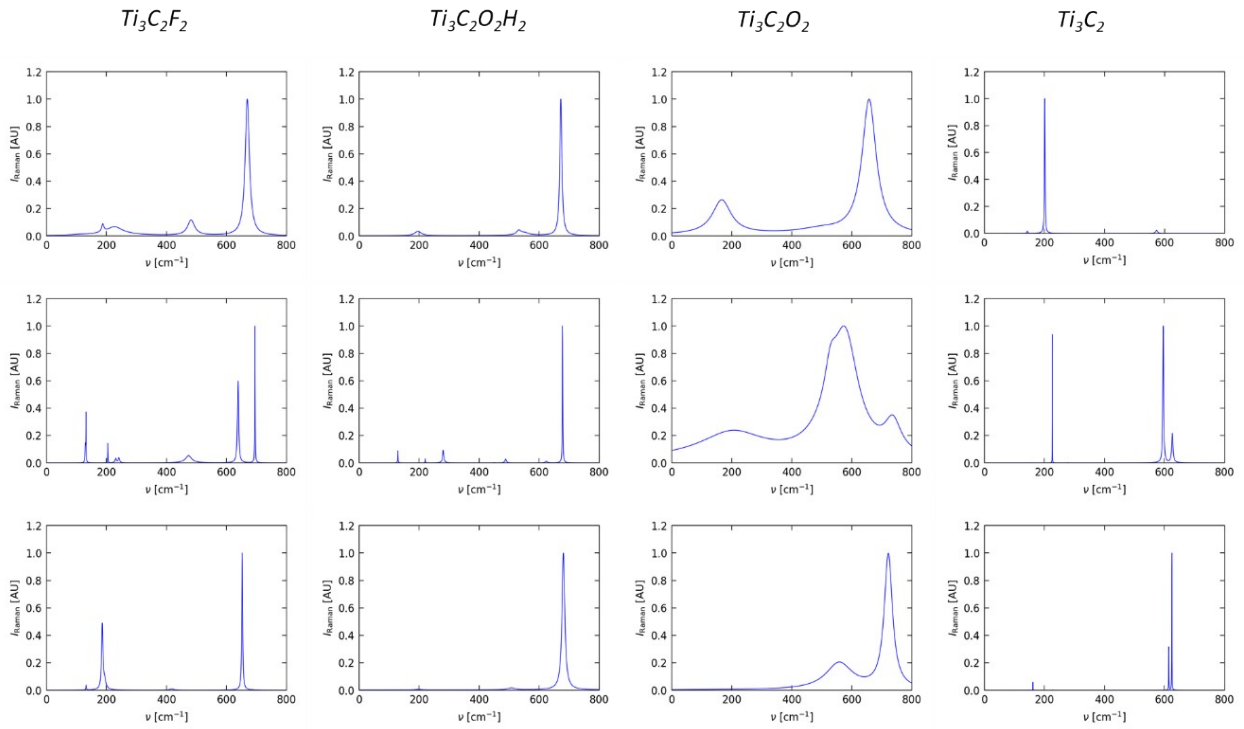

Figure S7. DFT calculated Raman spectra at 300K from the optimized unit cell structure. Linewidths are obtained from a high-quality Phono3py calculation [1]. From left to right: $Ti_3C_2F_2$, $Ti_3C_2O_2H_2$, $Ti_3C_2O_2$, Ti_3C_2. From top to bottom: (an electron removed from DFT simulation cell), neutral charge, reduction (an electron added to DFT simulation cell).

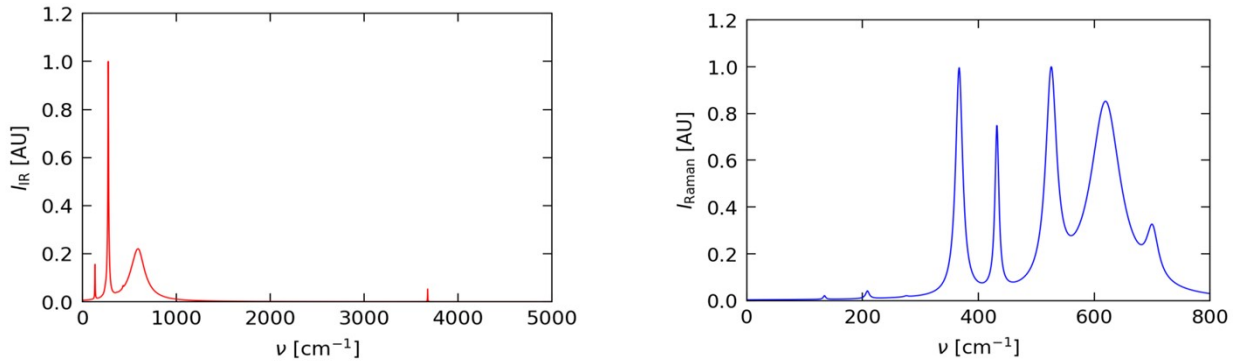

Figure S8. Simulated IR spectrum and Raman spectrum result at 300K for optimized unit cell structure $Ti_3C_2(OH)(H)$, whose linewidths are obtained from a high-quality Phono3py calculation.[1]

Table S7. Effects of surface charge on bond lengths (Å). Ti_1 is the surface Ti atom, Ti_2 is the inner Ti atom.

System	Bond			
	Ti1-C1	oxidation	neutral	reduction
Ti_3C_2		2.061	2.049	2.054
$Ti_3C_2F_2$		2.148	2.07	2.047
$Ti_3C_2(OH)_2$		2.143	2.081	2.074
$Ti_3C_2O_2$		2.325	2.191	2.153
	C1-Ti2	oxidation	neutral	reduction
Ti_3C_2		2.269	2.217	2.213
$Ti_3C_2F_2$		2.225	2.191	2.193
$Ti_3C_2(OH)_2$		2.217	2.192	2.191
$Ti_3C_2O_2$		2.182	2.157	2.165

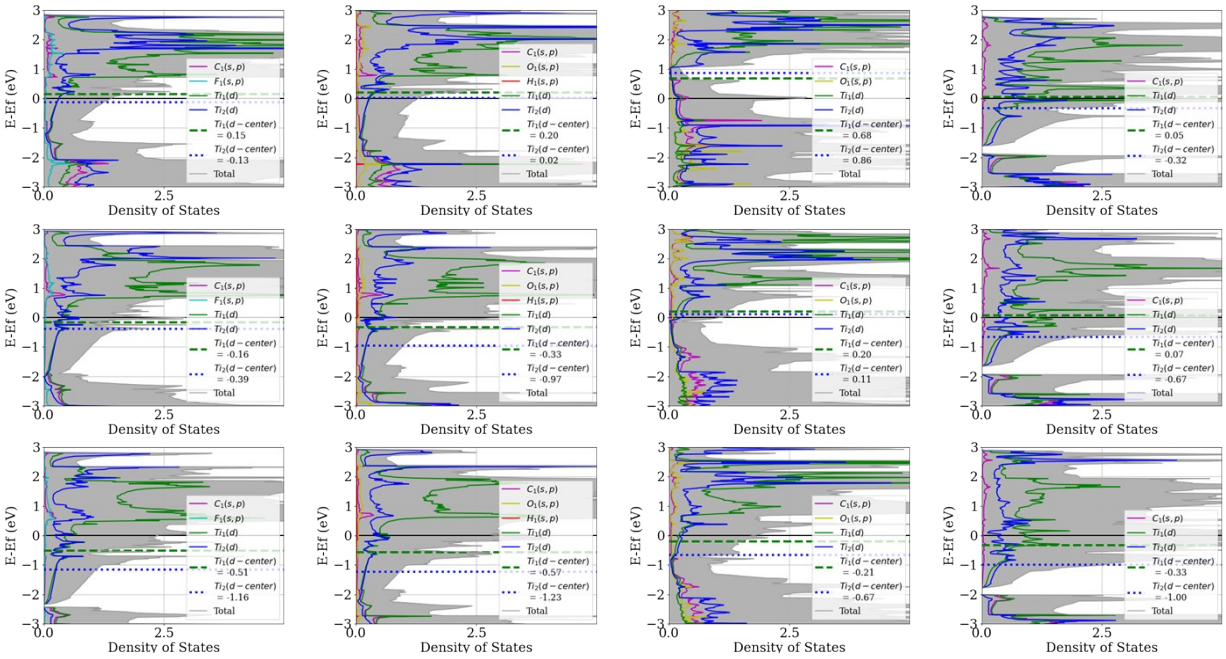

Figure S9. Individual atomic projected density of states and d-band center, where the Fermi energy is located at zero. From left to right: $Ti_3C_2F_2$, $Ti_3C_2O_2H_2$, $Ti_3C_2O_2$, Ti_3C_2. From top to bottom: oxidation (remove an electron from simulation cell), neutral charge, reduction (add an electron to simulation cell). where Ti_1 is outer Ti atom, Ti_2 is the inner Ti atom.

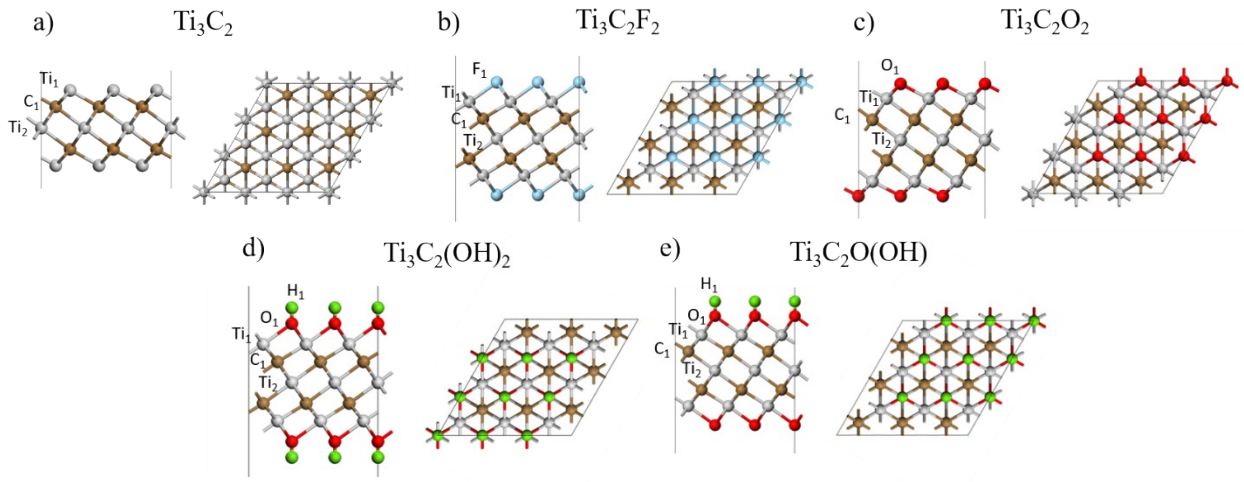

Figure S10. Illustration of ICOOP calculation with optimized unit cell structures (represented with 3 x 3 supercell), side view, top view, and its supercell structure. Gray, red, brown, blue, and green represent Ti, O, C, F, H, respectively.

Table S8. ICOHP (in eV) of selected pairs of $Ti_3C_2T_x$ slabs. ICOHP integrals are calculated from CHOP energies up to the Fermi level. Negative values indicate strong bonds, the more negative, the stronger the bonds. Positive values indicate weak bonds. Ti_1 is outer Ti atom, Ti_2 is the inner Ti atom. The atoms are numbered as in Figure S9.

System	Atom pair	ICOHP (eV) Oxidation	ICOHP (eV) Neutral charge	ICOHP (eV) Reduction
Ti_3C_2	C1-Ti1	-3.829	-3.482	-3.054
	C1-Ti2	-2.542	-2.640	-2.295
$Ti_3C_2O_2$	C1-Ti1	-2.304	-2.776	-2.701
	C1-Ti2	-0.025	-0.036	-0.031
	O1-Ti1	-4.508	-3.880	-3.362
$Ti_3C_2O_2H_2$	C1-Ti1	-3.373	-3.530	-3.467
	C1-Ti2	-0.026	-0.031	-0.031
	O1-Ti1	-2.538	-2.121	-2.056
	H1-O1	-8.517	-7.703	-7.453

$Ti_3C_2F_2$	C1-Ti1	-3.425	-3.730	-3.586
	C1-Ti2	-0.024	-0.029	-0.023
	F1-Ti1	-2.415	-1.925	-1.631

Table S9. Details of COHP calculations: Absolute charge spilling (%) value for $Ti_3C_2T_x$ terminated group (max is 2.38% / range from 0.88%-2.38%)

	Oxidation	Neutral charge	Reduction
	abs. charge spilling: (%)	abs. charge spilling: (%)	abs. charge spilling: (%)
Ti_3C_2	1.55%	1.60%	2.14%
$Ti_3C_2O_2$	1.02%	1.05%	2.38%
$Ti_3C_2O_2H_2$	0.98%	1.20%	2.05%
$Ti_3C_2F_2$	0.89%	0.97%	1.29%

Basis sets for each atom in the COHP calculations:

C: 2p 2s
H: 1s
O: 2p 2s
Ti: 3d 3p 3s 4s
F: 2p 2s

Table S10. Absolute and relative internal energies of optimized slabs, in eV. The relative energies are calculated with respect to the energy of the pristine slab, Ti_3C_2.

System	Internal energy, eV			Relative internal energy, eV		
	Oxidation	Neutral	Reduction	Oxidation	Neutral	Reduction
$Ti_3C_2O_2$	-57.837	-63.680	-61.929	-19.102	-19.795	-19.198
$Ti_3C_2O_2H_2$	-68.297	-70.190	-67.787	-29.562	-26.305	-25.056
$Ti_3C_2F_2$	-54.816	-58.368	-55.801	-16.081	-14.483	-13.070
$Ti_3C_2O_2H$		-66.878			-22.993	
Ti_3C_2	-38.735	-43.885	-42.731			

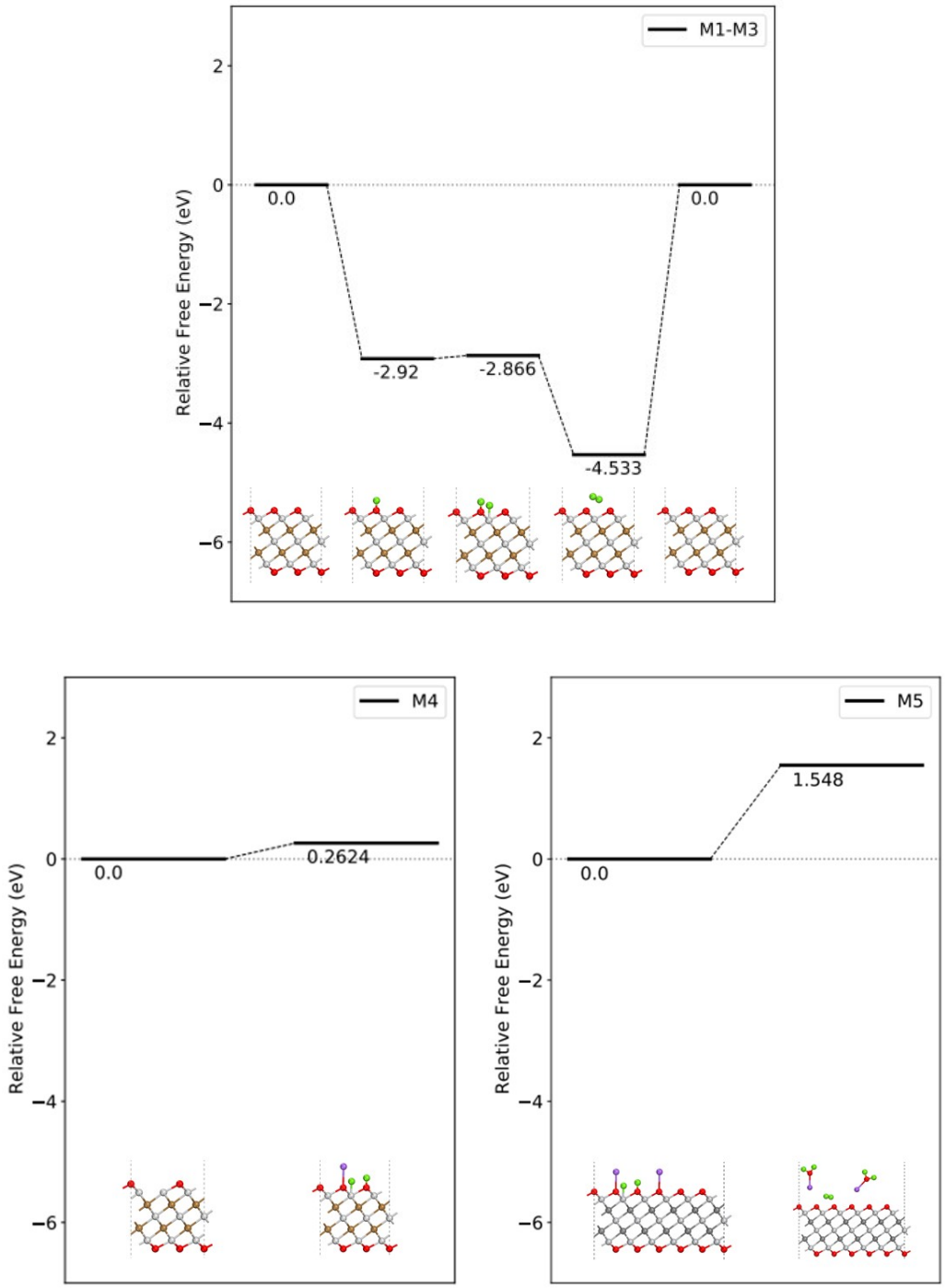

Figure S12. Energy profiles for the proposed mechanisms. Top: Reactions (1) to (3). Bottom: Reactions (4) and (5).

Note: All the DFT data for Raman and IR are available from the authors upon request.

References

1 A. Togo and I. Tanaka, *Scripta Materialia*, 2015, **108**, 1-5.